

# A Physics-Based TCAD Framework for the Noise Analysis of RF CMOS Circuits under the Large-Signal Operation

Sung-Min Hong, Raseong Kim, Chan Hyeong Park\*, Hong Shick Min, and Young-June Park  
 School of Electrical Engineering and Computer Science and NSI-NCRC,  
 Seoul National University, Seoul 151-744, Korea  
 E-mail : hi2ska2@isis.snu.ac.kr

\* School of Electronics Engineering, Kwangwoon University, Seoul 139-701, Korea

**Abstract**—A general TCAD framework for the large-signal (LS) noise analysis of RF CMOS circuits has been developed employing an efficient preconditioner for generalized minimal residual (GMRES) method. In this framework the influence of the noise sources inside the devices on the output noise of the circuit is calculated using the conversion Green's function (CGF) technique. We expect that the newly-developed TCAD framework can provide a physics-based and efficient LS noise analysis under a mixed device-circuit environment. As an application, noise behaviors of a single-balanced down-conversion mixer has been simulated using this framework.

## I. INTRODUCTION

As the technology scaling continues, CMOS has become a viable RF technology for portable wireless systems. In modern wireless communication systems, mixer and local oscillator circuits are the key circuits in frequency conversion. Understanding and analysis of noise performance of these circuits under large-signal (LS) conditions has become crucial in the successful low-noise design of CMOS RF ICs. Therefore, we need an accurate and physics-based TCAD framework for noise analysis of RF circuits under LS conditions.

In the circuit simulation, many circuit simulators either for time domain analysis or frequency domain analysis have been developed, based upon the compact MOSFET model (e.g., SPICE, Agilent ADS, and Cadence SpectreRF), and these simulators are widely used for noise analysis of CMOS RF circuits. However, in the mixed-mode device-circuit simulation [1], only a few attempts have been made to simulate the LS noise behaviors of very simple circuits [2], [3], and we still have to develop more efficient mixed-mode device-circuit simulators for an accurate LS noise analysis of practical RF CMOS circuits.

In this paper, we report a general TCAD framework of a mixed-mode device-circuit solver for the LS noise analysis of RF CMOS circuits. The harmonic balance (HB) method is employed to solve the state equations, which give the working points of the devices in the circuit considered. The iterative matrix solver, GMRES [4], is adopted as a matrix solver, and an efficient preconditioner, which can be effective even for a system with high distortion, is introduced. The paper is organized as follows. Section II is devoted to description of the HB simulation framework, which includes the matrix solver, GMRES, together with a very efficient preconditioner for GMRES. In Section III, the conversion Green's function (CGF) technique, which is employed to calculate the influence

of the noise sources inside the devices on the output noise of the circuit, is discussed. As an application of our TCAD framework, a detailed noise analysis of a single-balanced down-conversion CMOS RF mixer circuit is presented in Section IV. Conclusions are summarized in Section V.

## II. FRAMEWORK FOR THE HARMONIC BALANCE METHOD

We consider a circuit system consisting of semiconductor devices and lumped circuit elements. A lumped circuit element can be fully characterized by its terminal voltages and currents. The semiconductor equations (Poisson's equation and continuity equations for electron and hole) for each device in the circuit are discretized as in the conventional device simulators [5]. Then the state variables for the system are the electric potential, the electron densities and the hole densities at every node of the spatially discretized devices, and the terminal voltages and currents of the lumped elements. The total number of the state variables is denoted by  $N_S$ . During the LS simulation, the noise sources inside the devices and the lumped elements are not included, and only the responses of the state variables due to the externally applied voltage sources will be considered. The externally applied voltages can be time-varying.

In the HB method, we assume that each of the state variables can be represented as a linear combination of  $N_H$  frequency components. From this assumption, each state variable can be determined completely from the values of each state variables at  $N_H$  sampling times. Now we derive the equations satisfied by the  $N_S N_H$  values of the state variables at  $N_H$  sampling times. First, we write down the  $N_S$  state equations for the circuit system in the time domain, which can be written as

$$f(x, \dot{x}) = f_1(\dot{x}) + f_2(x) - b = 0, \quad (1)$$

where  $f$  is the residual vector for  $N_S$  state variables,  $x$  denotes the vector for the state variables in the time domain,  $\dot{x}$  is the time derivative of  $x$ ,  $b$  is the vector for the externally applied voltages, and  $f_1$  and  $f_2$  are usually nonlinear functions. Since Eq. (1) should be satisfied at each of  $N_H$  sampling times, we can constitute from Eq. (1) the  $N_S N_H$  equations satisfied by the  $N_S N_H$  values of the state variables at  $N_H$  sampling times, given by

$$f^*(x^*, \dot{x}^*) = f_1^*(\dot{x}^*) + f_2^*(x^*) - b^* = 0, \quad (2)$$

where  $f^*$  is the residual vector for the  $N_S N_H$  state variables,  $x^*$  is the vector for the  $N_S N_H$  values of the state variables,  $\dot{x}^*$  is the time derivative of  $x^*$ , and  $b^*$  is the vector for the values of the external voltages at  $N_H$  sampling times. Let  $X$  be the vector for the  $N_S N_H$  unknown quantities in the frequency domain corresponding to the vector  $x^*$ , then we have

$$x^* = \Gamma^{-1} X, \quad \dot{x}^* = \Gamma^{-1} \Omega X, \quad (3)$$

where  $\Gamma$  and  $\Gamma^{-1}$  are the discrete Fourier transform matrix pair for  $x^*$  and  $X$ , and  $\Omega$  is a block-diagonal matrix representing the frequency domain equivalent of the time derivative operation. Substituting Eq. (3) into Eq. (2), we obtain the  $N_S N_H$  equations satisfied by the  $N_S N_H$  unknown quantities in the frequency domain.

These equations can be solved by the Newton iteration method as follows. Let  $X_0$  be a tentative solution for a certain Newton loop and  $\Delta$  be the correction vector for  $X_0$ , then  $\Delta$  can be obtained from the following equation of

$$A_1 \Gamma^{-1} \Omega \Delta + A_2 \Gamma^{-1} \Delta = -f^*(\Gamma^{-1} X_0, \Gamma^{-1} \Omega X_0), \quad (4)$$

where  $A_1$  and  $A_2$  are given by  $\partial f_1^* / \partial \dot{x}^*|_0$  and  $\partial f_2^* / \partial x^*|_0$ , respectively.  $A_2$ , which is a matrix with size of  $N_S N_H \times N_S N_H$ , is composed of  $N_H$  smaller matrixes with size of  $N_S \times N_S$ . Each of the  $N_H$  smaller matrixes is the quasi-static Jacobian of the system for the  $N_S$  state variables, evaluated at each of the  $N_H$  sampling times. Eq. (4) can be rewritten as

$$(A_1 T + A_2) \delta = -f^*(\Gamma^{-1} X_0, \Gamma^{-1} \Omega X_0), \quad (5)$$

where  $T \equiv \Gamma^{-1} \Omega \Gamma$  is a matrix representing the time derivative operation for  $x^*$  in the time domain,  $\delta \equiv \Gamma^{-1} \Delta$  is an update vector in the time domain.

Since the square matrix of  $A_1 T + A_2$  in Eq. (5) has a size of  $N_S N_H \times N_S N_H$ , which is usually too big to be handled by a direct matrix solver such as UMFPAK [6] in the practical circuits, we take some efficient approaches [7], [8] to solve Eq. (5) through Krylov subspace method such as GMRES [4] or QMR [9]. In these approaches the most important procedure is to choose an appropriate preconditioner for Eq. (5). The block-diagonal preconditioner adopted in [7], [8] has been known to be very suitable for a system with low distortion, but this preconditioner is not suitable to a RF circuit where the power level is high. In this paper we use the GMRES, and we choose  $A_2$  as a preconditioner because it has been known that  $A_2$  can be a very good approximation of  $A_1 T + A_2$  specially at low frequencies which are much below the cutoff frequencies of the devices in the circuit considered [10] and because frequencies of our interest are much below the cutoff frequencies of the MOSFETs in the RF circuit. Since as discussed before,  $A_2$  is composed of  $N_H$  smaller matrixes with size of  $N_S \times N_S$ , each of which is the quasi-static Jacobian of the system for the  $N_S$  state variables, evaluated at each of the  $N_H$  sampling times,  $A_2$  can be decomposed into  $N_H$  "small" blocks. These small blocks with size of  $N_S \times N_S$  can be stored independently. This decomposition will save the memory usage and the workload for the matrix backsolve

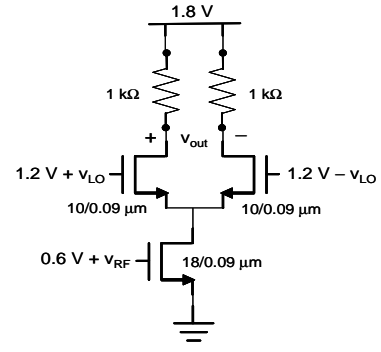


Fig. 1. Circuit schematic of the single-balanced down-conversion mixer.  $N_S$  is about 24,000 and  $N_H$  is set at 21. The LO is a sinusoidal voltage source of 1 GHz.

required during the preconditioning process. We expect that the time for one GMRES inner solve increases almost linearly as  $N_H$  increases. Adoption of  $A_2$  as a preconditioner and decomposition of  $A_2$  into  $N_H$  small blocks are distinctive features in our framework. We also note that our solution is exact in the sense that we use the exact Jacobian instead of an approximate one. Based on the LS working points obtained through the HB method, we will calculate the power spectral density of the output noise of the circuit.

### III. CONVERSION GREEN'S FUNCTION TECHNIQUE FOR LARGE-SIGNAL NOISE ANALYSIS

We exploit the conversion Green's function technique for the LS noise analysis of the circuit as in [2], [11], [12]. Let  $G_\alpha(\mathbf{r}, \omega)$  for  $\alpha = \psi, n, p$  be the CGFs for the given output variable based on the noiseless working points obtained in Section II as in [2], [11], [12], then the sideband amplitudes of the output noise variables are linearly related to the various sideband amplitudes of the microscopic noise sources inside the devices through the CGFs. The sideband correlation matrix (SCM) of two output noise variables, e.g. the short-circuit noise currents at terminals  $i$  and  $j$ , can be written as [2], [11], [12]

$$S_{i_n, i, i_n, j}(\omega) = \sum_{\alpha, \beta = \psi, n, p} \int_{\Omega} d\mathbf{r} G_\alpha(\mathbf{r}, \omega) \mathbf{K}_{\gamma_\alpha, \gamma_\beta}(\mathbf{r}, \omega) G_\beta^\dagger(\mathbf{r}, \omega), \quad (6)$$

where  $\mathbf{K}_{\gamma_\alpha, \gamma_\beta}(\mathbf{r}, \omega)$  is the SCM of the local noise sources for spatially uncorrelated microscopic fluctuations,  $\gamma_\alpha$  denotes the microscopic noise source included as a forcing term in equation  $\alpha$  ( $\alpha = \psi, n, p$  denote Poisson's, electron, and hole continuity equations, respectively),  $\dagger$  denotes the complex conjugate and transpose, and  $\omega$  is the sideband angular frequency. The direct extension of the generalized adjoint approach [13] allows a numerically efficient evaluation of the CGFs.

### IV. SIMULATION RESULTS AND DISCUSSION

Simulation has been carried out on the single-balanced down-conversion mixer whose output signal is taken as a differential voltage between the drain terminals of two LO MOSFETs. The circuit schematic considered in the simulation

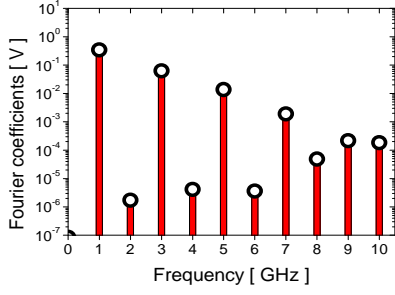


Fig. 2. Magnitudes of Fourier coefficients of the mixer output voltage. The amplitude of the LO signal is 0.15 V.

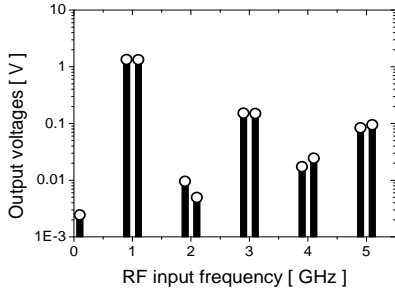
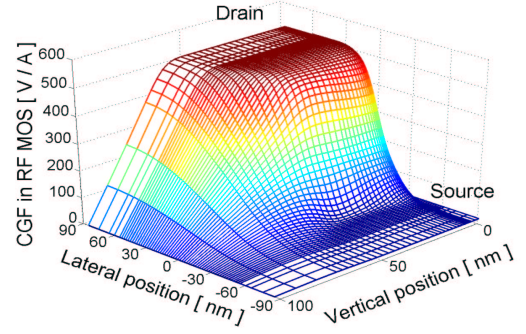


Fig. 3. Response of the mixer output voltage at 0.1 GHz to the unit RF input signal at various frequencies.

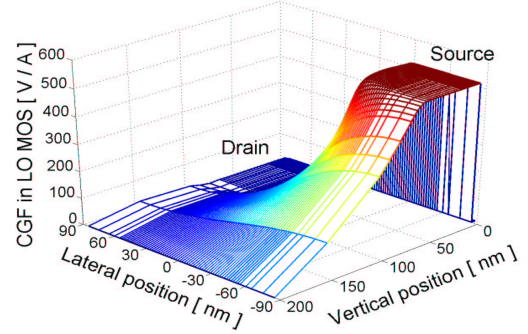
is shown in Fig. 1. The mixer consists of two resistors and three nMOSFETs and  $N_S$  is about 24,000. Since  $N_H$  is set at 21, the whole system has about half a million unknowns. The amplitude and frequency of the sinusoidal LO voltage source is 0.15 V and 1 GHz, respectively. In the noise calculation, only the diffusion noise sources are considered.

First we perform the LS mixer simulation where only the LO voltage source is imposed. In Fig. 2, the magnitudes of the Fourier coefficients of the mixer output voltage are shown. Based upon the simulated LS solution, the response of the linear periodically time-varying system to the RF input signal is evaluated. We select 0.1 GHz as the sideband frequency. Fig. 3 depicts the response of the mixer output voltage at 0.1 GHz due to the unit RF input signal at various frequencies. From this figure, we can see that the conversion gain for the 1.1 GHz RF signal is 1.33 V/V.

Let  $G(\mathbf{r}, n)$  be the CGF due to the noise source in the electron continuity equation at  $(n + 0.1)$  GHz, when the observation variable is the mixer output noise voltage at 0.1 GHz. Fig. 4 shows  $G(\mathbf{r}, 1)$ 's for the RF port MOSFET and for the left LO port MOSFET. In the case of the RF port MOSFET, the noise sources in the drain side of the channel give stronger impact on the mixer output noise. On the other hand, for the LO port MOSFET the noise sources in the source side of the channel have stronger impact on the mixer output noise, because in the case of the LO port MOSFET only the



(a)



(b)

Fig. 4.  $G(\mathbf{r}, 1)$  for (a) the RF port MOSFET and (b) the left LO port MOSFET.  $G(\mathbf{r}, 1)$  is the CGF due to the noise source in the electron continuity equation at 1.1 GHz, when the observation variable is the mixer output noise voltage at 0.1 GHz.

noise sources in the source side of the channel go through the down-conversion process. Furthermore,  $G(\mathbf{r}, 0)$  for the LO port MOSFET is shown in Fig. 5. The influence of the noise source only in the drain side of the LO port MOSFET is found to be dominant because the frequency conversion does not take place in this case. Fig. 6 shows magnitudes of the diagonal element of the integrand in Eq. (6) at a down-converted frequency (IF frequency) of 0.1 GHz for the left LO port MOSFET and either for the RF port MOSFET. The power spectral density of the mixer output noise voltage is calculated to be  $20.2 \text{ (nV)}^2/\text{Hz}$ , among which 55 % comes from the RF port MOSFET and the rest comes from the LO port MOSFETs (we neglected the noise from two resistors). Finally, we calculate the mixer output noise voltage at various LO amplitudes (0.1, 0.15, 0.2, 0.25 V). Fig. 7 shows the simulated mixer output voltages in the time domain. Also the conversion gains and power spectral densities of the mixer output noise voltage are shown in Fig. 8.

## V. CONCLUSIONS

In this work, we have developed a general TCAD framework for the LS noise analysis of CMOS RF circuits. The noise characteristic of the RF CMOS single-balanced down-conversion mixer has been simulated. We expect that this

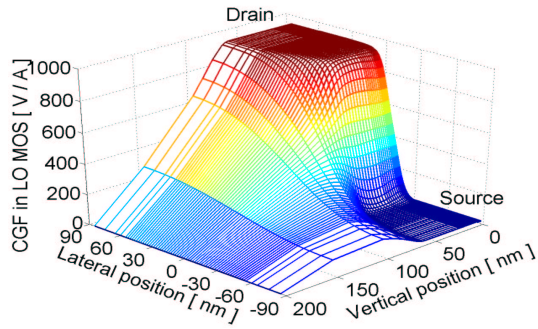
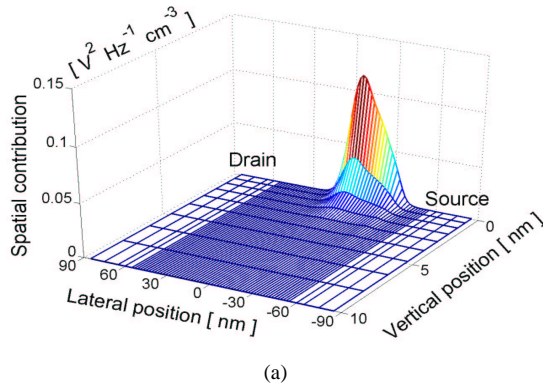
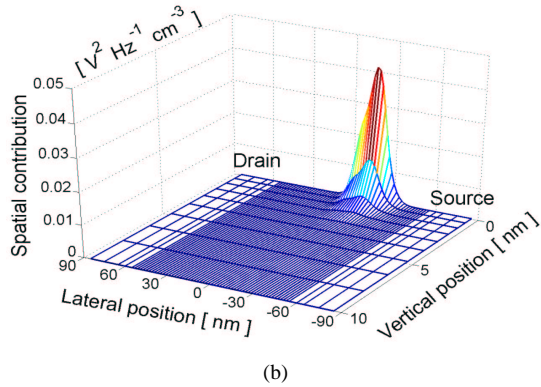


Fig. 5.  $G(r, 0)$  for the left LO port MOSFET.



(a)



(b)

Fig. 6. Magnitudes of the diagonal element of the integrand in Eq. (6) at a down-converted frequency (IF frequency) of 0.1 GHz for (a) the left LO port MOSFET and (b) the RF port MOSFET.

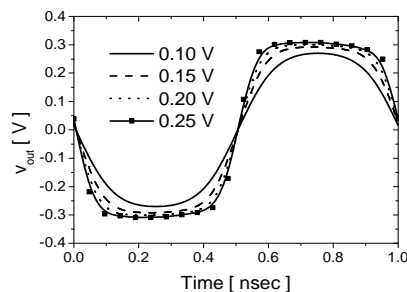


Fig. 7. Mixer output voltage in the time domain at various LO amplitudes.

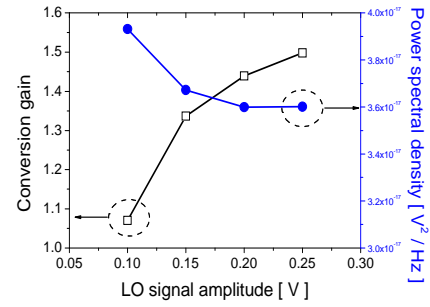


Fig. 8. Conversion gains and power spectral densities of the mixer output noise voltage as a function of the LO amplitude.

framework can be extended for the physics-based and efficient LS noise analysis of general RF CMOS circuits.

#### ACKNOWLEDGEMENT

This work was supported by the National Core Research Center program of the Korea Science and Engineering Foundation (KOSEF) through the NANO Systems Institute at Seoul National University. C. H. Park's work was supported by the National Program for Tera-Level Nanodevices of the Ministry of Science and Technology as one of the 21st century Frontier Programs.

#### REFERENCES

- [1] J. G. Rollins *et al.*, "Mixed-mode PISCES-SPICE coupled circuit and device solver," *IEEE Trans. Computer-Aided Design*, vol. 7, pp. 862–867, 1988.
- [2] F. Bonani, *et al.*, "A TCAD approach to the physics-based modeling of frequency conversion and noise in semiconductor devices under large-signal forced operation," *IEEE Trans. Electron Devices*, vol. 48, pp. 966–977, 2001.
- [3] J. E. Sanchez, *et al.*, "Two-dimensional semiconductor device simulation of trap-assisted generation-recombination noise under periodic large-signal conditions and its use for developing cyclostationary circuit simulation models," *IEEE Trans. Electron Devices*, vol. 50, pp. 1353–1362, 2003.
- [4] Y. Saad *et al.*, "GMRES: a generalized minimal residual method for solving nonsymmetric linear systems," *SIAM Journal on Scientific and Statistical Computing*, vol. 7, pp. 856–869, 1986.
- [5] *ATLAS Users Manual*, SILVACO International, Santa Clara, CA, 2000.
- [6] T. A. Davis, *UMFPACK Version 4.0 User Guide*, Dept. of Computer and Information Science and Engineering, Univ. of Florida, Gainesville, FL, 2002.
- [7] B. Troyanovsky, "Frequency domain algorithms for simulating large signal distortion in semiconductor devices," Ph.D. dissertation, Stanford Univ., Stanford, CA, 1997.
- [8] P. Feldmann, *et al.*, "Efficient frequency domain analysis of large nonlinear analog circuits," in *Proc. of IEEE Custom Integrated Circuits Conference*, 1996, pp. 461–464.
- [9] R. Freund, *et al.*, "Iterative solution of linear systems," *Acta Numerica*, pp. 57–100, 1992.
- [10] Y. Hu *et al.*, "A comparison of non-quasi-static and quasi-static harmonic balance implementations for coupled device and circuit simulation," in *Proc. of IEEE Custom Integrated Circuits Conference*, 2003, pp. 99–102.
- [11] F. Bonani, *et al.*, "Physics-based simulation techniques for small- and large-signal device noise analysis in RF applications," *IEEE Trans. Electron Devices*, vol. 50, pp. 633–644, 2003.
- [12] F. Bonani *et al.*, *Noise in Semiconductor Devices. Modeling and Simulation*. Heidelberg, Germany: Springer-Verlag, 2001.
- [13] F. Bonani, *et al.*, "An efficient approach to noise analysis through multidimensional physics-based models," *IEEE Trans. Electron Devices*, vol. 45, pp. 261–269, 1998.